

K^{*0} resonance production at wide p_T range in pp collisions at $\sqrt{s} = 13$ TeV (2015 data)

Kunal Garg¹

1. University of Catania

Email: kgarg@cern.ch

Abstract

Short lived resonances are good probes to study the properties of strongly interacting matter produced in high energy heavy ion collisions. In particular, the resonance $K^*(892)^0$ is important because of its very short lifetime which is comparable to that of the fireball. So the decay daughters are expected to undergo re-scattering and re-generation processes, which could modify the resonance characteristic properties such as its mass, width and yield at low transverse momentum (p_T). Here we present preliminary results from the measurement of $K^*(892)^0$ resonance in pp collisions at $\sqrt{s} = 13$ TeV reconstructed via its hadronic decay channel ($K^{*0} \rightarrow K^\pm + \pi^\mp$).

1 Introduction

ALICE (A Large Ion Collider Experiment) is one of seven detector experiments at the Large Hadron Collider at CERN. ALICE focuses on the physics of strongly interacting matter at extreme energy densities. It is optimised to study heavy ion collisions with a centre of mass energy at some TeV per nucleon. At this energy scale, it's expected that matter breaks down into constituent free quarks and gluons and thus is termed Quark-Gluon Plasma (QGP). The existence of QGP is vital for understanding Colour Confinement and Chiral Symmetry Restoration.

QCD is the theory of strong interactions, a fundamental force describing the interactions between quarks and gluons which make up hadrons such as the proton, neutron and pion. QCD is a non-abelian gauge theory with symmetric group $SU(3)$. Colour is the analog of charge in QED and gluons are the force carrying particles.

The QCD phase transition can be investigated in laboratory by reproducing by means of ultra-relativistic collisions, the temperature, pressure and energy density conditions that lead to the QGP formation. The product of the collision is a fireball in local thermal equilibrium that rapidly expands and cools down. The development of the fireball after collisions, although much faster, is believed to reproduce the evolution stages of the early Universe.

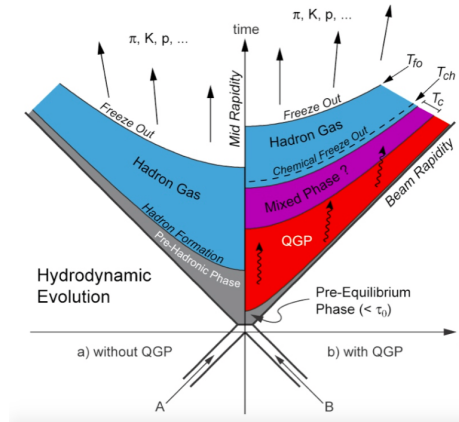


Figure 1: Evolution of the fireball

In the right part of Fig. 1, the evolution of the fireball going through the QGP phase is schematically displayed[1]. The fireball expansion leads to decrease in the temperature and density. When the temperature reaches the critical value (T_{cr}), the system undergoes a transition to hadronic phase. This temperature may or may not be equal to the temperature of the chemical freeze out which is the moment when inelastic collisions stop. Further expansion leads to kinetic freeze-out which is the moment when also the elastic collisions stop. Resonance particles like the K^{*0} have lifetimes comparable to that of the fireball itself. Thus studying resonances can give us information about timescale between chemical and kinetic (thermal) freeze out [2]. The Large Hadron Collider (LHC) at CERN provides collisions of protons at centre of mass energies up to 13 TeV per nucleon and of Pb-Pb up to $\sqrt{s_{NN}} = 5$ TeV. Thanks to its Particle Identification (PID) performances, ALICE

detector is well suited to reconstruct low and high p_T hadronic resonances.

Normally pp collisions are used to build reference for large systems. The effects due to the presence of medium are checked by comparing the pp collision results to the Pb-Pb ones. However ALICE measurements during RUN 1 data taking period have pointed out, in high-multiplicity pp events, features typical of QGP formation which were expected only in PbPb collisions. Moreover analysis of pp collisions permit us to study Parton Distribution Function (PDFs) at low -x.

In this work we will present results for $K^{*0}(892) + \bar{K}^{*0}(892)$ (in the following indicated with K^{*0}) production in pp collisions at $\sqrt{s} = 13$ TeV. K^{*0} decays into a $\pi^\pm + K^\mp$ with a branching ratio of 0.66. K^{*0} has a mass equal to 0.896 GeV/ c^2 and decays with a Breit-Wigner width of 0.048 GeV[3].

2 Event and Track Selection

2.1 Data Set

This analysis is done with the data of pp collisions at centre of mass energy $\sqrt{s} = 13$ TeV collected during 2015.

Data: **LHC15f/pass2/ESDs**

Run Numbers used are:

225026, 225031, 225035, 225037, 225041, 225043, 225050, 225051, 225052, 225106, 225305, 225307, 225309, 225313, 225314, 225322, 225576, 225578, 225579, 225586, 225587, 225707, 225708, 225709, 225710, 225716, 225717, 225719, 225753, 225757, 225762, 225763, 225766, 225768, 226062, 226170, 226220, 226225, 226444, 226445, 226452, 226466, 226468, 226472, 226476, 226483, 226495, 226500.

2.2 Event Selection

- **kINT7 trigger:** This trigger should correspond to a logical AND between trigger inputs from V0A and V0C detectors.
- Standard Physics Selection.
- Is InComplete DAQ check.
- Pileup Rejection using AliAnalysisUtils::IsPileUpEvent().
- SPD Clusters vs. Tracklets Check using AliAnalysisUtils::IsSPDClusterVsTrackletBG() with default parameters.
- Event has a track or SPD primary vertex identified.
- SPD vertex-z resolution < 0.25 cm.
- SPD vertex dispersion < 0.04 cm.
- z-position difference between track and SPD vertex < 0.5 cm.
- vertex-z position : $|v_z| < 10$ cm.

2.3 Track Selection

Standard set of track selection cuts were used.

- $0.15\text{GeV}/c < p_T$
- $-0.8 < \eta < 0.8$
- Reject kink daughters.
- Minimum number of rows crossed in TPC is 70.
- TPC χ^2 clusters < 4.0
- ITS χ^2 clusters < 36.0
- $|\text{DCA}|_z < 2 \text{ cm}$
- $(\text{DCA})_r < 0.0105 + 0.0350p_T^{-1.01}$
- Pair rapidity $< |0.5|$

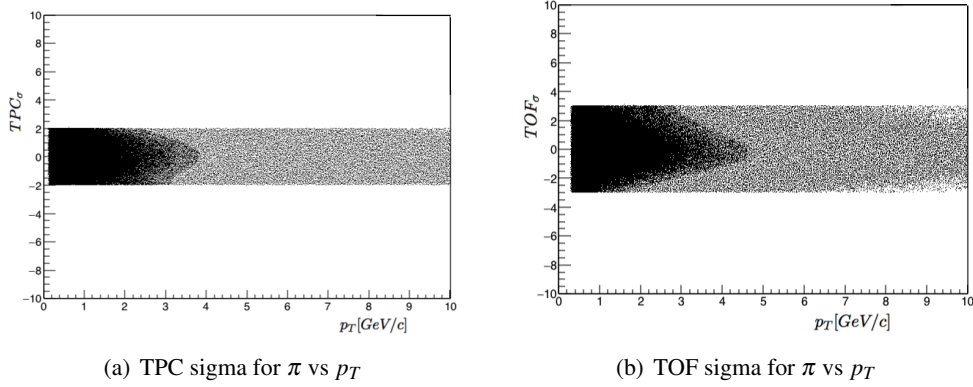
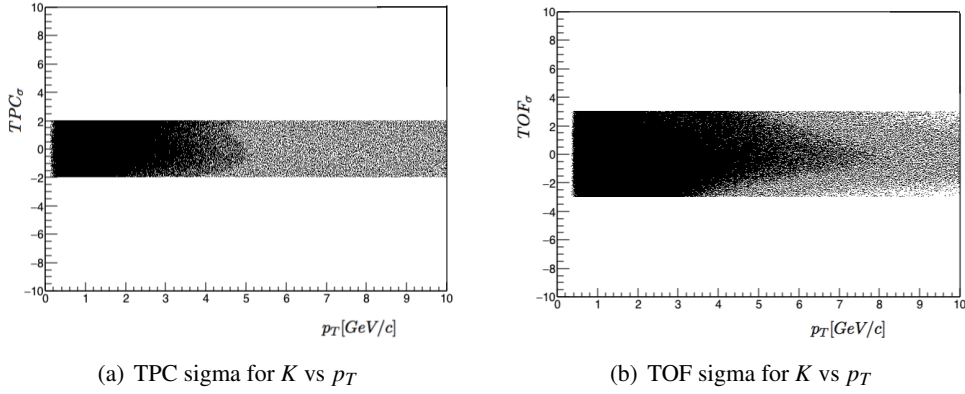
2.4 Particle Identification

The daughter particles of K^{*0} are charged kaons and pions and they can be identified by using Time Projection Chamber (TPC) and Time Of Flight (TOF) detectors. Particle identification in TPC[4] is performed by measuring the specific energy loss (dE/dx) in the detector gas. The energy loss is described by the Bethe-Bloch function:

$$\left\langle \frac{dE}{dx} \right\rangle = \frac{4\pi N e^4}{mc^2} \frac{Z^2}{\beta^2} \left(\ln \frac{2mc^2 \beta^2 \gamma^2}{I} - \beta^2 - \frac{\delta(\beta)}{2} \right), \quad (1)$$

where mc^2 is the rest energy of the electron, Z the charge of the projectile, N the number density of electrons in the traversed matter, e the elementary charge, β the velocity of the projectile and I is the mean excitation energy of the atom. A truncated mean that rejects the 40% largest cluster charges is built, resulting in a Gaussian dE/dx response. The measured energy loss is compared to standard energy loss (Bethe-Bloch function) for different particles to identify them. The dE/dx resolution ranges between 5 – 8% depending on the track inclination angle and drift distance, the energy loss itself and the centrality of the collisions due to the different detectors.

The TOF detector is based on Multigap Resistive Plate Chamber technology. It measures the time of flight of particles with an intrinsic resolution of ~ 80 ps. The expected flight time for each particle species is calculated during the reconstruction, and then PID is performed via a comparison between the measured and expected times. Both pions and kaons are selected by a cut of $|N\sigma_{\text{TPC}}| < 2.0$ with a TOF veto of $|N\sigma_{\text{TOF}}| < 3.0$. TOF veto means that the TOF cut is applied only for cases where the track matches a hit in the TOF. (see Fig. 2 and 3)

Figure 2: PID for π Figure 3: PID for K

3 Signal Extraction using Event Mixing

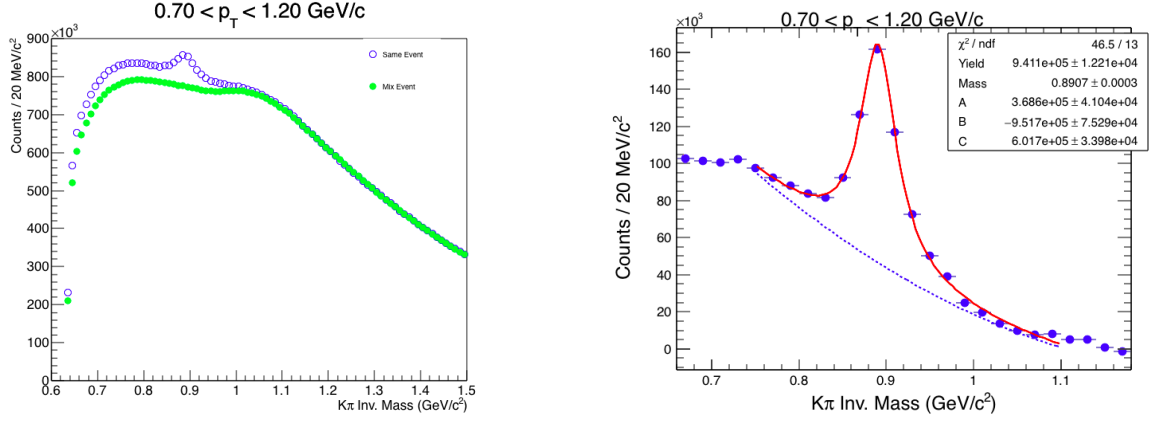
To extract the yields of K^{*0} mesons in each p_T bin, the following procedure is used[5]. The invariant-mass distribution of unlike-charge pairs from the same event is computed. The combinatorial background is estimated by event-mixing technique and subtracted from the unlike-charge distribution.

In event-mixing technique, the combinatorial background is constructed through the invariant mass of pions and kaons of different events having similar z-vertex, and multiplicity. For the reconstruction, we mix 5 events which have z-vertex difference within 1 cm and multiplicity difference within 5. The mixed event is normalised by the same event distribution in the region of invariant mass of 1.1 to 1.3 GeV/ c^2 . (see Fig. 4a) The signal is obtained by subtracting the mixed event combinatorial background from the same event kaon - pion invariant mass distribution. (see Fig. 4b)

After subtraction of combinatorial background, a certain amount of background is left under the K^{*0} signal, which is known as residual background. The source of this residual background may be:

1. correlated real $K\pi$ pairs from other resonance decay.
2. correlated but misidentified $K\pi$ pairs.

The invariant mass calculated from misidentified pairs can not be subtracted away by mixed event background and it remains as a residual background.



(a) Unlike-sign invariant mass distribution (open blue circles) and invariant mass obtained by mixed events (green circles) for transverse momentum range 0.7 – 1.20 GeV/c. The distribution obtained by event mixing technique is normalised in the range 1.1 – 1.3 GeV/c²

(b) Unlike-sign invariant mass distribution after background subtraction for the transverse momentum range 0.7 – 1.2 GeV/c. Red curve represents the result of the fit (see text). Blue dashed curve represents the background estimated by a polynomial (see text)

Figure 4:

4 Mass

The background-subtracted unlike-charge invariant mass distribution is fitted by a function given by the sum of a non-relativistic Breit-Wigner function and a second order polynomial.

$$\frac{Y}{2\pi} \frac{\Gamma_0}{(M_{K\pi} - M_0)^2 + \frac{\Gamma_0^2}{4}} + \text{Polynomial}$$

where M_0 and Γ_0 are the mass and width of the K^{*0} , $M_{K\pi}$ is $K\pi$ invariant mass. The parameter Y gives the Breit-Wigner area. The mass values obtained for the different p_T bin are reported in Fig. 5.

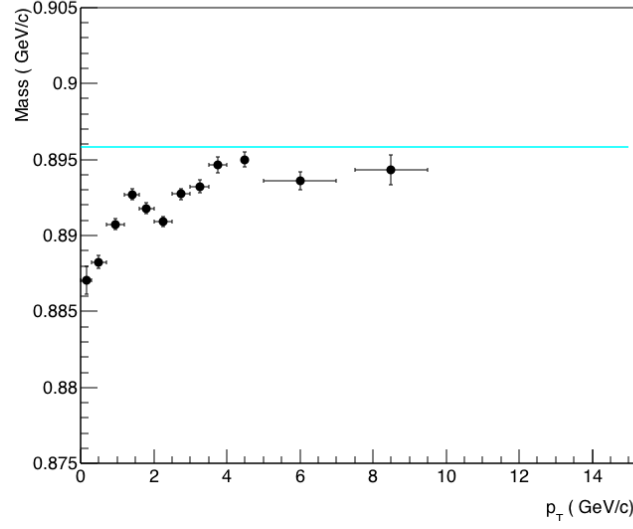


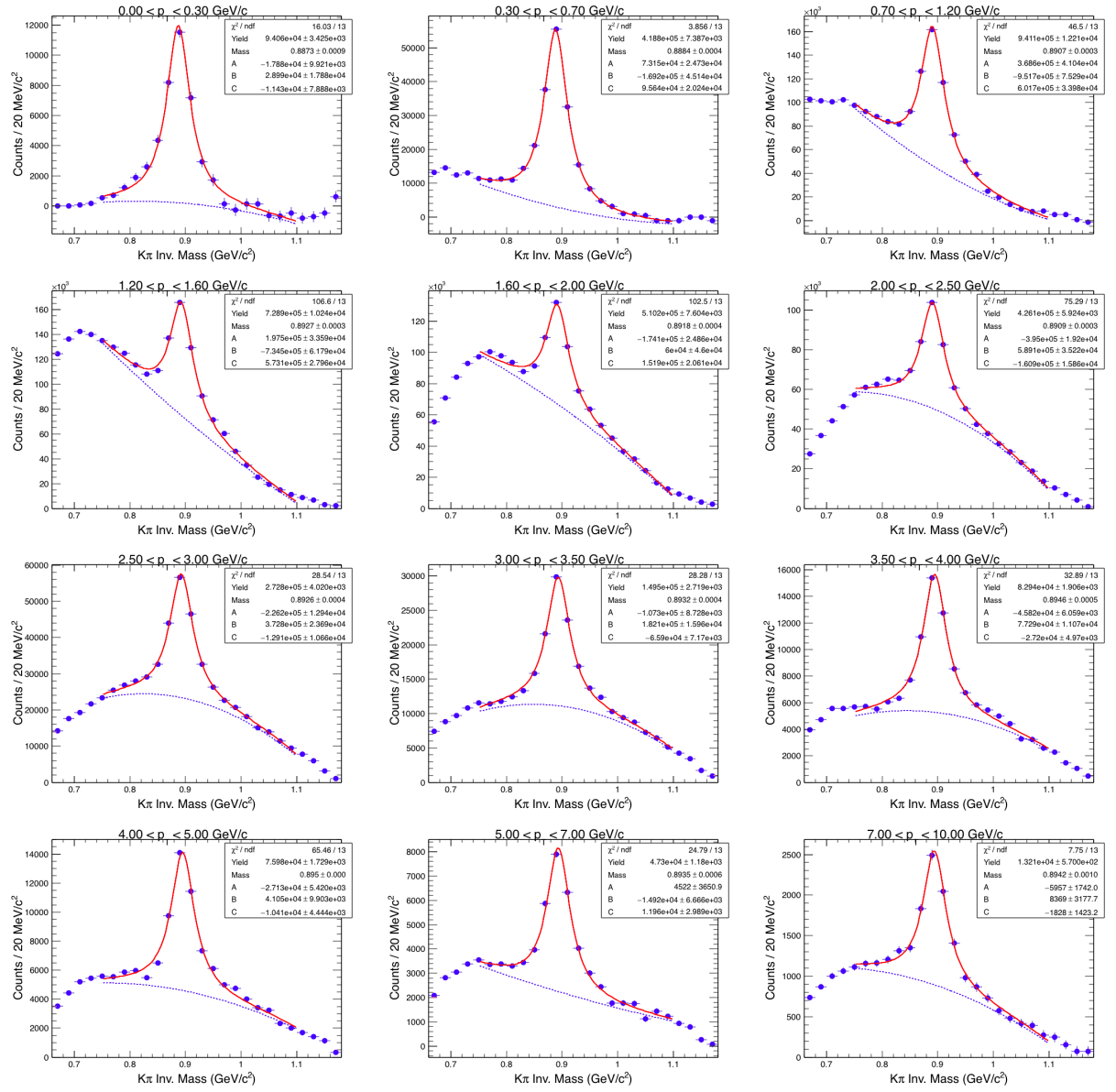
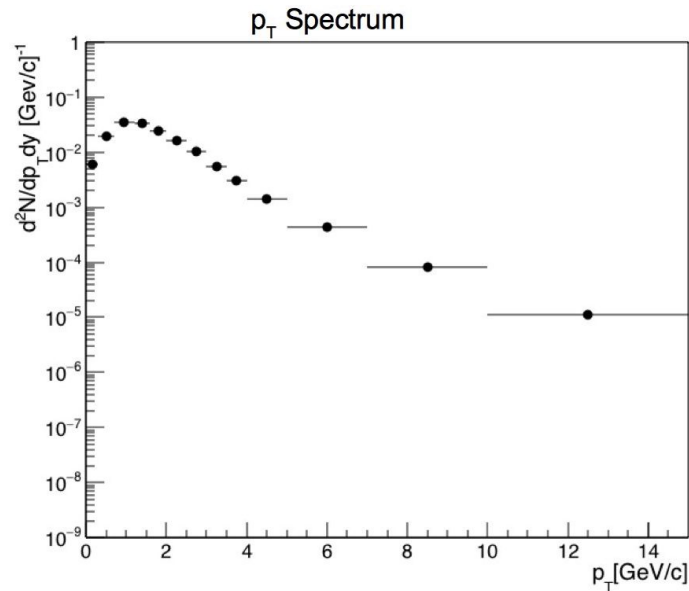
Figure 5: Mass vs. p_T . The line represent the $K^*(892)^0$ PDG mass value.

5 Raw Yield Extraction

K^{*0} raw yield for each p_T bin is obtained by fitting the invariant mass distribution while fixing the width value to the PDG one ($0.0474 \text{ GeV}/c^2$) [3]. The raw yield is obtained from the Y parameters of the Breit-Wigner function.

The yield has been estimated in 13 p_T bins lying between : 0, 0.3, 0.7, 1.2, 1.6, 2.0, 2.5, 3.0, 3.5, 4.0, 5.0, 7.0, 10.0, 15.0 GeV/c . The invariant mass distributions and the fit results for the different p_T bins are shown in Fig. 6.

The raw yield p_T spectrum is shown in Fig. 7.

Figure 6: Fitting results from different p_T regions for BW+ Polynomial function

6 Monte Carlo

6.1 Efficiency x acceptance of K^{*0}

Acceptance is defined as the percentage of generated particles whose final states are geometrically included in the detector. Efficiency takes into account detector limitations that for a given particle depend on the mass, charge, momentum etc.

We use Monte Carlo productions to estimate our efficiency x acceptance. In our present case, we used the Monte Carlo production LHC15g3a3 which was generated using PYHTIA8[6] - Monash 2013. PYHTIA is an example of event generators which are software libraries that generate simulated high-energy particle physics events. In most processes a factorisation of the full process into individual problems is possible, these individual processes are calculated separately, and the probabilistic branching between them is performed using Monte Carlo methods. The final-state particles generated by event generator is fed into the detector simulation, allowing a precise prediction and verification for the entire system of experimental setup.

The acceptance times efficiency is defined as the ratio of the number of reconstructed K^{*0} mesons having decay daughters ($K^\pm \pi^\mp$) that passes through the track cuts which are used in real data analysis to the number of generated K^{*0} with same decay daughter in rapidity interval ± 0.5 .

$$\epsilon_{rec} = \frac{N_{reconstructed}}{N_{generated}}$$

The uncertainty in ϵ_{rec} is calculated using the Bayesian approach. The choice of bayesian approach is motivated by the fact that the events of numerator and denominator are correlated. The standard deviation for the efficiency $\epsilon_{rec} = k/n$, where the numerator k is a subset of the denominator n , is:

$$\sigma_\epsilon = \sqrt{\frac{k+1}{n+2} \left(\frac{k+2}{n+3} - \frac{k+1}{n+2} \right)}$$

The K^{*0} acceptance x efficiency distribution as a function of p_T is shown in Fig. 8.

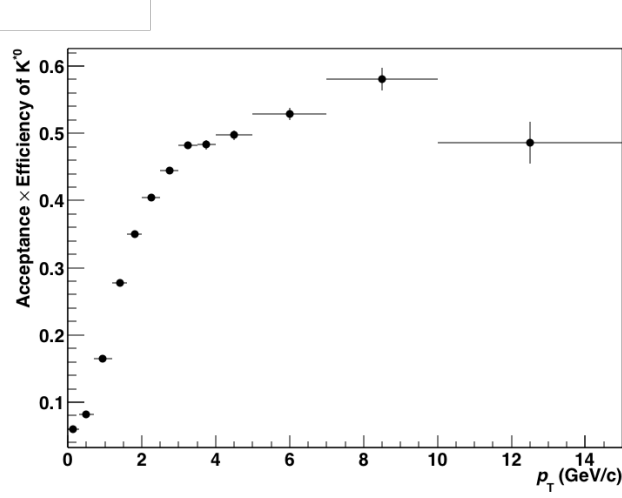


Figure 8: Efficiency x Acceptance vs p_T for K^{*0}

6.2 Corrected p_T spectrum

To extract the yield, raw counts were corrected for the decay branching ratio(BR), and for the losses due to pion/kaon in-flight decays, geometrical acceptance and detector efficiency(eff) ($N_{cor} = \text{Raw Counts} / \text{BR} \times \text{eff}$). Absolute resonance yield in inelastic collisions is estimated using the following formula:

$$\frac{d^2N}{dp_T dy} = \frac{\text{Raw Counts}}{N_{MB} \times BR \times dp_T \times dy \times eff} \times f_{norm} \times f_{SL}$$

where N_{MB} is the number of the minimum bias trigger selected by the event cuts, BR is the branching ratio (which is the fraction of particles decaying in the desired decay mode with respect to the total number of particles decaying), eff is the acceptance x efficiency of reconstruction. The factor $f_{norm} = 0.852^{+0.062}_{-0.03}$ is efficiency for trigger selection for inelastic pp collisions. The factor $f_{SL} = 0.931264$ accounts for the signal loss introduced by the requirement that a primary vertex must be reconstructed and be in the range of ± 10 cm.

The correct value for f_{norm} for Run2 data is not yet accurately known so we use the value from Run1[5].

The obtained p_T spectrum for K^{*0} is shown in Fig.9

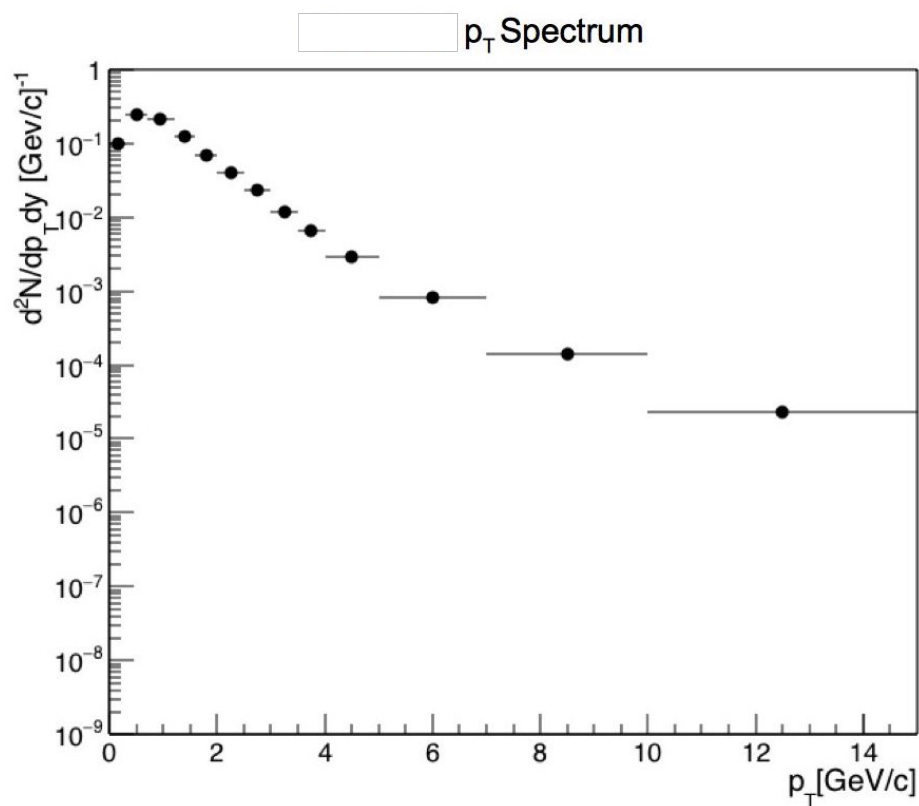


Figure 9: Transverse momentum spectrum of K^{*0} produced in pp collisions at $\sqrt{s} = 13$ TeV

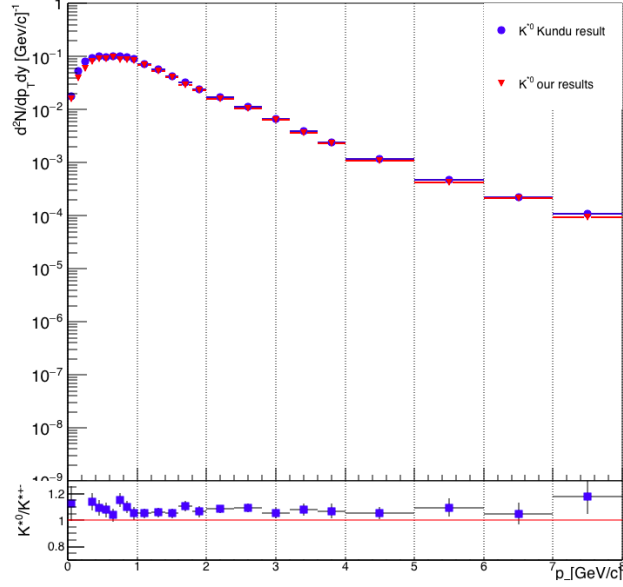


Figure 10: Spectra comparison with approved results.

Fig. 10 is the comparison between the official p_T spectrum (blue symbols)[5] and the ones obtained in this analysis (red symbols). The results are divided by a factor of 2 to account for $K^{*0} + \bar{K}^{*0}$ and corrected for branching ratio and efficiency only.

7 Summary

We have studied K^{*0} production in pp collision at $\sqrt{s} = 13$ TeV data in different p_T bins. The p_T distribution of raw yield has been corrected for efficiency, branching ratio, vertex and trigger efficiency. The mass has been extracted as a function of p_T . This study has been done as a way to learn the analysis methods which will be employed to study the $K^{*\pm}$ resonance which is our primary source of interest.

References

- [1] F. Bellini's PhD thesis for University of Bologna. (2013)
- [2] C. Markert *et al.* Strange Hadron Resonances: Freeze-Out Probes in Heavy-Ion Collisions. (arXiv:hep-ph/0206260)
- [3] J. Beringer *et al.* (PDG), PR D86, 010001 (2012)
- [4] J. Alme *et al.* Nucl Instrum Meth A 622 (2010) 316367
- [5] ALICE Collaboration. <https://aliceinfo.cern.ch/Notes/node/469>
- [6] T. Sjöstrand *et al.* Phys. Comm. 178 (2008) 852